Biophys J BioFAST, published on April 20, 2007 as doi:10.1529/biophysj.106.101766

Conformation of the EPEC Tir protein in solution: investigating the impact of serine phosphorylation at positions 434/463

Paul R. Race, Alexandra S. Solovyova & Mark J. Banfield[#]

Institute for Cell and Molecular Biosciences, Faculty of Medical Sciences, Newcastle University, Framlington Place, Newcastle upon Tyne, NE2 4HH. UK

[#]Author for correspondence

Running title: Solution structure studies of EPEC Tir

Keywords: circular dichroism, analytical ultracentrifugation, natively unfolded protein, structural-rearrangement, bacterial pathogenesis, mutagenesis.

Abstract

The translocated intimin receptor (Tir) is a key virulence factor of Enteropathogenic *E. coli* (EPEC) and related bacteria. During infection Tir is translocated via a type III secretion system into host intestinal epithelial cells, where it inserts into the target cell membrane and acts as a receptor for the bacterial adhesin intimin. The effects of phosphorylation by cAMP-dependent kinase at two serine residues (Ser434 and Ser463) within the C-terminal domain of Tir, which may be involved in mediating structural/electrostatic changes in the protein to promote membrane insertion or intermolecular interactions, have previously been investigated. This study has focused on defining the conformation of Tir in solution and assessing any conformational changes associated with serine phosphorylation at positions 434/463. In addition to phosphorylated protein, combinations of Ala (unphosphorylatable) and Asp (phosphate-mimic) mutations of Ser434 and Ser463 have been generated and a range of techniques (SDS-PAGE, circular dichroism spectroscopy, analytical ultracentrifugation) used to further dissect the structural role and functional implications of changes in residue size/charge at these positions. The results have shown that under physiological NaCl concentrations Tir is a monomer and adopts a highly elongated state in solution, consistent with a natively unfolded conformation. Despite this, perturbations in the structure in response to buffer conditions and the nature of the residues at positions 434 and 463 are apparent, and maybe functionally relevant.

Introduction

Infection with the gram negative bacterium enteropathogenic *E. coli* (EPEC) is a major cause of infantile diarrhoea in the developing world (1, 2). EPEC infection is characterised by destruction of host cell intestinal microvilli, actin rearrangement within epithelial cells and the formation of a raised platform or pedestal at the site of bacterial attachment (3). EPEC utilise a type III secretion system (TTSS) to deliver a series of protein effectors, directly into target epithelial cells. The translocated intmin receptor (Tir), a 56 kDa protein essential for EPEC virulence, becomes inserted into the plasma membrane of host epithelia cells following translocation through the TTSS (4). Following membrane insertion *in vivo*, Tir adopts a structure comprising N- and C-terminal domains on the cytosolic face of the membrane, linked via two transmembrane helices to an extracellullar domain which mediates intimin binding (5, 6). Recently the protein, which can be expressed and purified in a soluble form, has been shown to insert directly into membranes from solution *in vitro* adopting a topology as found *in vivo* (7).

Tyrosine phosphorylation plays an important role in EPEC Tir function with modification of Tyr474 essential for recruitment of the Nck adaptor molecule and actin nucleating machinery which results in pedestal formation (8, 9). A role for phosphorylation of Tyr454 in recruitment of cytoskeletal proteins and pedestal formation has also been proposed (10). EPEC Tir resolves on SDS-PAGE gels at a higher molecular mass (~78 kDa) than would be predicted from its sequence, which has been interpreted as the protein retaining some residual structure under these conditions (4). On translocation into mammalian cells Tir undergoes changes in apparent molecular mass resulting in protein isolated from infected cell membranes running at ~90 kDa on SDS-PAGE gels (4). These observations have led to the use of anomalous shifts on SDS-PAGE gels as probes for the conformational state of Tir in solution, revealing that changes in apparent molecular mass are mediated by serine phosphorylation (11) and can be mimicked *in vitro* by phosphorylation of Ser434 and Ser463 residues with cAMP-dependent protein kinase (PKA, (12)). Tir is also a substrate for PKA *in vivo* (11, 12). As phosphorylation of tyrosine residues within Tir has no effect on its apparent molecular mass (11, 12) the observed shifts cannot be fully accounted for by electrostatic effects of charge alteration on the protein (as discussed in (12)). Although Tir has recently been shown to insert directly into membranes in the absence of modification or accessory factors *in vitro*, it remains an attractive proposal that serine phosphorylation may act as a trigger or facilitator of Tir insertion into membranes *in vivo*. This could be mediated either directly through conformation/electrostatic changes promoting insertion or indirectly by assisting interactions with accessory factors.

One concern with the use of phosphorylated proteins for molecular/structural analysis is sample homogeneity, especially where multiple phosphorylation sites exist. The mutation of serine residues to Asp or Glu to mimic the effects of phosphorylation has become a well-established technique (13, 14). Of the amino acids, Asp/Glu best retain the shape and charge of phosphorylated serine residues. Using mutagenesis rather than enzymatic phosphorylation ensures homogeneity in the sample and allows the effects of individual phosphorylation events to be studied. When combined with alanine mutants (which are not phosphorylatable) and phosphorylation assays of the native protein (15), a detailed picture of the effects of phosphorylation can be obtained.

One interpretation of the anomalous migration of Tir in SDS-PAGE gels is that the protein may adopt a natively unfolded/disordered state in solution. This would be consistent with recent studies showing that natively unfolded proteins give apparent molecular masses 1.2-1.8 times

higher on SDS-PAGE gels than would be expected from the sequence, or measured by mass spectrometry (16). Recently, a number of studies have used circular dichroism (CD, a measure of the secondary structure content in proteins (16)), gel filtration (shape of protein (i.e asymmetry/elongation) expressed in terms of hydrodynamic (Stokes) radius (R_s) (17)) and small-angle scattering (radius of gyration (16, 18, 19)) to characterise natively unfolded proteins. For example, the value of R_s in relation to the mass of the protein is usually determined by gel filtration or dynamic light scattering and appears to be the one of the major indicative parameters for the protein to be recognised as intrinsically unfolded/disordered (16, 20).

Analytical ultracentrifugation (AUC) has recently been used for mass determination of natively unfolded proteins (21, 22). Sedimentation equilibrium studies gave an accurate value of protein molecular weight that was unaffected by its shape. The sedimentation velocity approach, which is a hydrodynamic technique, contains information about both protein mass and shape. Ordinarily one-dimension sedimentation velocity data treatment gives a value for the protein mass which is affected by its shape (usually the mass is under-estimated for elongated particles, especially if a mixture of species is present). Recently, a method for two-dimension treatment of sedimentation velocity has been proposed (23) which allows for determination of protein molecular mass and shape (expressed in terms of friction coefficient (f/f_0) or R_s) independently. Therefore, this approach can be particularly useful in characterising natively unfolded proteins adopting extended conformations in solution.

In this study a set of mutants has been generated to probe the effects of serine phosphorylation at positions 434 and 463 on the solution structure of EPEC Tir. Within a C-terminal domain construct (cTir) both Ser434 and Ser463 have been mutated to Ala or Asp in all combinations. Additionally, a double Asp mutant (Ser434Asp/Ser463Asp) has been generated in the full length protein (FL-Tir). These mutants are potentially useful tools for further study of Tir function where fine control of the phosphorylation state of these residues is important (for instance, studies of protein/membrane interaction). However, to be useful tools the mutations should mimic the effects of phosphorylation on the structure of Tir. A combination of SDS-PAGE and phosphorylation assays (to track changes in apparent molecular mass), CD spectroscopy and AUC (sedimentation velocity method) have been used to characterise the conformations of cTir and FL-Tir in solution and investigate structural changes following modification at the Ser434 and Ser463 positions. The results reveal that both FL-Tir and its C-terminal domain are monomeric and adopt highly elongated conformations at physiological conditions. This fact, combined with the limited amount of secondary structure observed for these proteins, suggests they adopt natively unfolded states in solution, which maybe important for function.

Materials and methods

Site directed mutagenesis

Ala and Asp mutants were generated in cTir by overlap extension PCR (24). Template plasmids (pET27b) containing the wild-type and S434A mutant cTir constructs were provided by Prof. B Kenny (Newcastle University). Primers were designed to span the regions encoding residues Ser434 and Ser463 and incorporate the appropriate mutation (base changes underlined): Ser434Asp, 5'-GAATAGACGTGATGATCAGGGGAGTGTT-3' (Forward), 5'-AACACTCCCCTGATCATCACGTCTATTC-3' (Reverse); Ser463Ala, 5'-GGCTCGGAATGCTCTATCGGCTCATCAG-3' (Forward), 5'-CTGATGAGCCGATAGAGCATTCCGAGCC-3' (Reverse); Ser463Asp, 5'-GGCTCGGAATGATCTATCGGCTCATCAG-3' (Forward), 5'-CTGATGAGCCGATAGATCATTCCGAGCC-3' (Reverse). Two PCR reactions were used to generate the upstream (T7 promoter primer and reverse primer encoding the mutation) and downstream (forward primer encoding the mutation and T7 terminator primer) regions of the coding sequence, with a third reaction used to generate the full length sequence (T7 promoter and T7 terminator primers, relevant products above as the template). Where generation of a second mutation was required the appropriate template DNA was used. Full length PCR products were cloned into pGEM-T (Promega) and mutations confirmed by sequencing. Coding regions were cut from pGEM-T with BamH1 and Nhe1 and ligated into pET27b, pre-digested with the same enzymes.

The Ser434Asp/Ser463Asp FL-Tir double mutant was generated in two steps using the Stratagene 'Quikchange' kit, following standard procedures. The same primers as above were used. Firstly the S434D mutant was generated, this construct was then used as template DNA for the second reaction generating the S463D mutation. The mutations were confirmed by DNA sequencing.

Protein expression and purification

pET27b plasmids encoding cTir and FL-Tir proteins were transformed into *E. coli* BL21 (DE3) cells for overexpression. Recombinant proteins were expressed and purified as described previously (7, 12), but with the addition of a final gel filtration step (HiLoad S75 16/60 column equilibrated in 20 mM Tris, 150 mM NaCl, pH 7.5) to ensure high purity. All protein concentrations were determined by absorbance at 280 nm using a theoretically derived extinction coefficient based on protein sequence.

Phosphorylation assays

Phosphorylated forms of cTir and FL-Tir were generated by incubating 0.3 mg of the substrate with 100 μM ATP and 3,000 units of PKA (NEB) in 1x PKA reaction buffer (NEB) at 30^{o}C for 4 hours. Control experiments (not shown) were the same, but with water substituted for PKA. Proteins were visualised using either 12% (cTir) or 8% SDS-PAGE (FL-Tir).

Circular Dichroism Spectroscopy

CD spectra were collected using a JASCO-810 spectropolarimeter, fitted with a Peltier temperature controller. Spectra of native and mutant cTir and FL-Tir were collected from 190-250 nm, using a 0.1 mm path-length cuvette, at 25 ^{o}C in 20 mM sodium phosphate, 150 mM

NaCl, pH 7.5. The concentration of each stock protein solution (~10 mg/ml) was determined by absorbance at 280nm followed by dilution to 0.2 mg/ml immediately prior to the experiments. Final spectra were generated as averages of 5 repeat scans, with appropriate protein-free buffer spectra subtracted. The data were plotted without smoothing using Excel™. The data were truncated to 190 nm on the wavelength axis corresponding to the value where the high tension voltage (HTV) rose above 600 V (the accepted measure of the signal:noise ratio for this machine, ensuring accurate measurements). The spectra were analysed with programs available at the DICHROWEB web server (http://www.cryst.bbk.ac.uk/cdweb/html/) (25). Secondary structure estimations were obtained using the Provencher and Glockner method (26).

Analytical ultracentrifugation

Sedimentation velocity (SV) experiments were carried out in a Beckman Coulter (Palo Alto, CA, USA) ProteomeLab XL-I analytical ultracentrifuge using both absorbance at 280 nm and interference optics. All AUC runs were carried out at the rotation speed of 48,000 rpm and experimental temperature 4°C. The sample volume was 400 µl for the SV experiments, and the sample concentrations ranged between 0.2 and 1.8 mg/ml. The partial specific volumes ($\bar{v}$) for the protein was calculated from the protein amino acid sequence, using the program SEDNTERP (27) and extrapolated to the experimental temperature following the method as described in (28). The density and viscosity of the buffer (20 mM Tris pH 7.5, 50/150 mM NaCl) at the experimental temperature was also calculated using SEDNTERP.

The distributions of sedimenting material was modelled as a distribution of Lamm equation solutions (29) where the measured boundary a(r,t) was modelled as an integral over differential concentration distributions c(s).

$$a(r,t) = \int c(s)\chi(s,D,r,t)ds + \varphi \qquad (1)$$

where φ is the noise component, r is the distance from the centre of rotation and t is time. The expression χ(s, D, r, t) denotes the solution of the Lamm equation (30) for a single species by finite element methods (31). Eq. 1 is solved numerically by discretisation into a grid of 200 sedimentation coefficients for both absorbance and interference data and the best-fit concentrations for each plausible species are calculated according to in a linear least squares fit (as implemented in the program SEDFIT (http://www.analyticalultracentrifugation.com)). The sedimentation velocity profiles were fitted using a maximum entropy regularisation parameter of p = 0.95. The weight average sedimentation coefficient was calculated by integrating the differential sedimentation coefficient distribution (32):

$$s_w = \frac{\int c(s)ds}{\int cds} \qquad (2)$$

Sedimentation coefficients were extrapolated to zero concentration and converted to standard conditions: those that would be measured at 20°C in water. The diffusion coefficient (D) corresponding to each sedimentation coefficient value was estimated from a weight-average frictional ratio $(f/f_0)_w$ (33)

$$D(s) = \frac{\sqrt{2}}{18\pi} kTs^{-1/2}[\eta(f/f_0)_w]^{-3/2}[(1-\bar{v}\rho)/\bar{v})]^{-1/2} \qquad (3)$$

The integration of the mass distribution c(M) was made similarly to as in Eq (2) to determine the weight average molecular mass of solute.

Two-dimensional "size-and-shape" distribution model ($c(s,f/f_0)$) was applied in order to determine precisely the value of molecular mass from sedimentation velocity data (23). In this model a differential distribution of sedimentation coefficients and frictional ratios (f_r, i.e. f/f_0) is defined as

$$a(r,t) = \iint c(s,f_r)\chi(s,D(s,f/f_0),r,t)dsdf_r \qquad (4)$$

where all symbols are the same as in Eq (1). In this model sedimentation coefficient and friction ratio (i.e. mass) for sedimenting species are fitted as independent variables. The numerical solutions of Eq (4) were obtained in discrete grid of 50 sedimentation coefficients and 10 values of f/f_0.

PONDR prediction for cTir/FL-Tir

Protein sequences were submitted to the PONDR web engine (www.pondr.com) using the neural network predictor VL-XT (34). Access to PONDR was provided by Molecular Kinetics (Indianapolis, IN).

Stokes radius calculations for cTir/FL-Tir

The theoretical Stokes radius (R_s) of the native (R_s^N) and fully unfolded (R_s^{Urea}) proteins were determined as described in (17):

$$\log R_s^N = 0.369 \times \log M_r - 0.254 \qquad (5)$$

$$\log R_s^{Urea} = 0.524 \times \log M_r - 0.657 \qquad (6)$$

Results

Phosphorylation of residues Ser434 and Ser463 in the EPEC Tir virulence protein by cAMP-dependent kinase (PKA) have been observed both *in vitro* and *in vivo* and are potentially important events for protein function (12). However, the detailed effects of these phosphorylation events on both protein structure and function remain to be fully determined. In an attempt to further characterise the effects of modification at these two sites, and generate tools for further study, a series of Ala and Asp mutations have been constructed and characterised *in vitro* using a number of techniques.

Changes in apparent molecular mass on SDS-PAGE

SDS-PAGE has previously been used as tool for visualising conformational dynamics within the cTir and FL-Tir proteins on phosphorylation (5, 11, 12). Fig. 1 shows an SDS-PAGE gel of unphosphorylated native and mutant cTir proteins revealing the Ser434Asp, Ser463Asp and Ser434Asp/Ser463Asp mutations result in significant increases in apparent molecular mass above that expected for a single residue change. As compared to the wild type protein, the increases in apparent molecular mass are ~4 kDa for Ser434Asp, ~6 kDa for Ser463Asp and ~12 kDa for the Ser434Asp/Ser463Asp double mutant (judged from the positions of the bands on the gel compared to the size marker). The shifts for the single point mutations differ suggesting they are not solely due to a change in the protein's charge. These shifts correlate well with previous *in vitro* and *in vivo* phosphorylation assays with both cTir and FL-Tir where progressive step-wise increases in apparent molecular mass have been attributed to successive phosphorylation of Ser434 and Ser463 (11, 12). The Ser434Ala/Ser463Asp double mutant resolves at a higher molecular weight than Ser434Asp/Ser463Ala, consistent with the pattern observed for the native/Asp mutants. The combined Ser434Asp/Ser463Asp mutant shows the greatest shift, closely approaching the change observed for the fully PKA-phosphorylated native cTir (below and, (12)).

The effect of the Ser434Asp/Ser463Asp mutant on the resolving properties of FL-Tir on SDS-PAGE is shown in Fig. 2d. As for the equivalent cTir mutant, the gel reveals a significant apparent molecular weight shift compared to the native protein.

Phosphorylation assays

The effects of PKA-mediated phosphorylation on wild-type and mutant cTir (detectable using the gel-shift analysis) are shown in Fig. 2, and reveal the modifications only involve residues Ser434 and Ser463. In any of the cTir mutant combinations where both residues are non-phosphorylatable no additional apparent molecular mass shifts are observed on SDS-PAGE gels. Where a single serine remains, incubation with PKA results in apparent molecular mass shifts showing this residue has been modified. This confirms that each serine residue is independently available for modification, and mutation of one site does not preclude phosphorylation of the second. Consistent with the observed effects of the Asp mutants in isolation, in the constructs where one of the Ser residues is replaced by an Asp the apparent molecular mass of the PKA-modified proteins on SDS-PAGE gels are higher than for the equivalent Ala substitutions.

Fig. 2d shows the resolving properties of native and phosphorylated FL-Tir in addition to the Ser434Asp/Ser463Asp mutant. The FL-Tir Ser434Asp/Ser463Asp mutant displays similar resolving properties to that of the phosphorylated wild type protein supporting, at least in this

assay, that the Ser434Asp/Ser463Asp mutant is an effective phosphorylation mimic. Attempts to phosphorylate the Ser434Asp/Ser463Asp mutant also suggests there are no further sites for PKA phosphorylation in FL-Tir (identifiable using this assay).

CD spectroscopy

Far-UV CD spectra of the cTir and FL-Tir proteins are shown in Figs. 4a and 4b respectively. For each of the cTir mutants, whilst essentially the same trace was obtained, two distinct classes are apparent. For three of the proteins (Ser434Ala, Ser434Asp/Ser463Ala, Ser434Asp/Ser463Asp) there is a slight shift to shorter wavelength and a deepening of the trough at just under 200nm (see Fig. 4a). Deconvolution of the spectra into secondary structure components reveals that the proteins largely adopt an 'unordered' structure in solution (66 - 74%, see Table 1) and that none of the mutations described result in a significant change in the secondary structure composition. Attempts to investigate the proteins' tertiary structure by near-UV CD revealed there was no significant spectroscopic signal in the 250 - 350 nm range, even at high protein concentrations. These results are consistent with previously published observations of native and phosphorylated cTir, where cTir was predicted to adopt a partially disordered or loosely packed structure (12).

Deconvolution of the CD spectra for the native and Ser434Asp/Ser463Asp FL-Tir is also presented in Table 1 (spectra shown in Fig. 4b). As for the comparison of the cTir WT and mutant proteins, these two spectra essentially overlay, indicating a very similar overall secondary structure composition. However, it is interesting to note that the shift to the left and deepening of the trough in the trace of the Ser434Asp/Ser463Asp mutant at approximately 205 nm compared to the native protein is consistent with the observed shift between the spectra of native and phosphorylated FL-Tir (12). This suggests the Ser434Asp/Ser463Asp mutant maybe mimicking any subtle changes phosphorylation has on the secondary structure content of FL-Tir. No significant near-UV CD spectra could be observed for FL-Tir at 10 mg/ml (180 μM); previously Tir was unstable at the concentrations required for this technique (12).

Hydrodynamic studies of cTir/FL-Tir by sedimentation velocity

Sedimentation velocity (SV) provides a qualitative measure for protein size and shape. Recent advances in SV data treatment enable accurate determination of molecular mass (to include the association state of macromolecules), where sedimentation equilibrium experiments were previously necessary (33, 35).

Each of the cTir mutants and the WT have been examined for heterogeneity using the continuous c(s) size distribution approach. One major dominant species was evident as a single peak centred around an apparent sedimentation coefficient ($s^{app}_{20,w}$) of 1.5 S for all the cTir mutants (in 150 mM NaCl). The peak corresponding to the major species of the cTir WT samples was displaced towards lower s-values (1.2 S). The integration of this peak gave a weight average sedimentation coefficient (extrapolated to zero concentration) for cTir mutants that varied between 1.46 S for the Ser434Ala/Ser463Ala mutant and 1.52 S for the Ser434Asp mutant (Fig. 3A and Table 2). All measured values of s are significantly less than those calculated for a sphere of the same molecular mass with typical hydration (2.46 S), which implies substantial elongation of cTir in solution.

The c(s) distribution of cTir WT in 50 mM NaCl had three easily distinguishable peaks centred at 1.7 S, 2.65 S and 4.25 S (Fig. 3B). Importantly, the peak positions are almost independent of

protein concentration, suggesting the timescale of exchange between oligomeric species is slow compared to the duration of the SV experiment (32). The overall integration of c(s) suggests that the oligomerisation of cTir WT in 50 mM NaCl is an equilibrium association process since the value of weight-average sedimentation coefficient for whole system increases with sample concentration (Fig. 3B, insert). Linear extrapolation to zero concentration gives sedimentation coefficient values under standard conditions of 1.78 ± 0.1 S for the monomeric species, 2.61 ± 0.14 S for dimer and 4.22 ± 0.09 S for tetramer. Interestingly, the sedimentation coefficient for the cTir monomer in 50 mM NaCl is much higher than the s value for the same sample in 150 mM NaCl. Conversion of the c(s) distribution to the c(M) distribution (data not shown) followed by peak integration yields a molecular mass of 18.5 ± 0.5 kDa for monomer, 39.7 ± 2.6 kDa for dimer and 68.2 ± 2.2 kDa for tetramer, which is in reasonable agreement with that predicted from the amino acid composition of the protein (19.8 kDa for monomer, 39.6 kDa for dimer and 79.2 kDa for tetramer, Table 2).

For some cTir mutants, minor species of lower molecular weight were observed on the continuous c(s)/c(M) distribution, resulting in inaccurate determination of molecular mass following peak integration. To compensate for this a two-dimensional distribution "mass-and-shape" model was applied to provide shape-independent estimation of the molecular mass from the SV data (Brown and Schuck 2006). This two-dimensional distribution $c(s,f_r)$ with following peak integration also includes the determination of the Stokes radius (R_s) of the particles from SV profiles. The theoretical calculations of R_s (see Materials and Methods) for cTir in a folded and unfolded state based on its molecular mass gave the values of 21.4 Å and 39.3 Å respectively. The experimentally determined values of R_s for cTir WT and all mutants ranged between 33.8 and 38.8 Å (see Table 2), again suggesting that they adopt an unfolded conformation in solution, consistent with the CD data. The most extended conformation was observed for cTir-WT in 150 mM NaCl while the most "compact" samples were the S434A/S463A and S43D/S463D mutants; the phosphorylated protein also seems to be more compact than wild type cTir (35.4 Å compared to 38.8 Å).

FL-Tir forms an essentially homogeneous monomeric species in solution as determined by AUC, with an s value of 2.65 (Fig. 3C, Table 2) and a molecular mass of 60.5 kDa ± 2.1 kDa. A small peak at ~ 4 S that may represent a dimeric species (or other form of aggregate) did not exceed 3% in solution. There were no significant changes observed in the hydrodynamic properties of FL-Tir following phosphorylation and no significant difference was observed between FL-Tir and the Ser434Asp/Ser463Asp mutant. However, the phosphorylated sample seems to possess a slightly more compact conformation as revealed by its sedimentation coefficient and Stokes radius. The calculated Stokes radius for FL-Tir was 32.1 Å for the folded and 69.8 Å for unfolded states respectively. The experimentally determined radius for native FL-Tir was 57 Å; the phosphorylated FL-Tir has an almost identical Stokes radius (56.2 Å). The Ser434Asp/Ser463Asp mutant was slightly more extended (62.7 Å).

Discussion

This study aimed to investigate the solution structure of EPEC Tir and determine whether the effects of PKA-mediated phosphorylation in the protein can be mimicked by site-directed mutagenesis. Both cTir and FL-Tir are shown to adopt natively unfolded conformations in solution. The importance of natively unfolded proteins in mediating protein-protein interactions is an emerging theme in molecular recognition. Within this context SDS-PAGE, CD spectroscopy and AUC have been used to characterise the solution structure of Tir constructs where Ser434 and Ser463 have been mutated to Ala and Asp, and these have been compared to both the native protein and the protein phosphorylated at these positions. Implications for the function of Tir are discussed.

cTir and FL-Tir are natively unfolded proteins in solution

Analysis of the structure of cTir and FL-Tir by CD spectrometry and AUC demonstrates experimentally that they adopt extended conformations in solution, with little tertiary structure. A low degree of compactness (i.e. high hydrodynamic radius of molecule) is an important characteristic in the definition of a natively unfolded state in solution (17). The experimentally determined hydrodynamic radii of cTir and FL-Tir in solution have been compared with both (a) proteins previously demonstrated to be natively unfolded and (b) proteins unfolded in 8 M urea (Table 3). The high similarity between the mass:hydrodynamic radius ratio observed for cTir and FL-Tir with these proteins provides further evidence that they adopt an essentially unfolded state in solution. Further, bioinformatic analysis of the amino acid composition of cTir reveals the protein contains 31% “disorder-promoting” residues (such as Pro, Glu, Ser and Gln (17, 36) and only 11% “order-promoting” residues (Tyr, Phe, Trp Ile and Leu; Cys is absent). The same analysis for FL-Tir reveals 28% “disorder promoting” and 14% “order promoting” residues. This reflects on the percentage of disordered structure predicted by PONDR (34) 78.4% for cTir and 67.6% for FL-Tir (Fig 5A). It is also worth noting that the amino acid sequence of FL-Tir contains four proline-rich clusters (either P-X-X-P or P-P/G sequences) which have a high propensity to form PPII-type helical structures (37).

Prior to adopting its final conformation as a integral transmembrane receptor Tir is (a) bound by a molecular chaperone (CesT) following overexpression in the bacteria (which protects the protein from degradation and may be involved in delivery of Tir to the type III secretion system) and (b) passes through the ‘needle’ of the type III translocon in an at least partially unfolded state. The protein is then predicted to be released into the cytoplasm where it inserts into the membrane. It would seem likely that the expressed protein described here represents this pre-insertion form, and this is natively unfolded, but soluble in solution. The importance of natively unfolded proteins in promoting efficient interactions with other molecules (for example in regulation and cell signalling) has recently been investigated (16, 20, 36, 38, 39). It is an attractive hypothesis that the natively unfolded state adopted by FL-Tir in solution maybe important for the structural transition into an integral membrane protein by providing an appropriate interaction surface or promoting penetration of the lipid bilayer due to exposed hydrophobic residues.

Bioinformatic analysis of the predicted regions of disorder in Tir (as generated by PONDR, Fig. 5) reveals the presence of a MoRF-like sequence (Molecular Recognition Feature (40, 41)) centred around residue Ser434. MoRFs are defined as short, loosely structured regions in proteins that are surrounded by largely disordered sequences (41), and have been implicated in molecular recognition events, particularly protein:protein interactions associated with cell

signalling and regulation. Upon binding their partners these MoRFs undergo disorder-order transitions. Additionally, it has been shown that a significant proportion of MoRFs contain a predicted phosphorylation site, and phosphorylation may be a common mechanism to modulate MoRF binding activity (41). The identification of a MoRF centred on the 434 region of Tir supports a role for this region in regulating intermolecular interactions with an as-yet unidentified binding partner, and suggests that phosphorylation of this residue may modulate binding affinity.

Oligomerisation of cTir in solution

Previously, when Tir proteins were prepared in 50 mM NaCl, it was shown that cTir existed in a monomer-dimer equilibrium (by AUC and native gels), with phosphorylation affecting the oligomerisation state of the protein; the implications for Tir function were discussed (12). In the present study protein preparations and experiments were conducted at more physiological NaCl concentrations (150mM in all buffers, also with an additional gel filtration purification step where a single peak was observed). At these salt concentrations, the AUC experiments reveal there is no change in oligomeric state (1) following cTir phosphorylation or (2) for any of the cTir variant proteins. Also, only single bands are seen on native gels for all samples (data not shown). If cTir samples are prepared in only 50 mM NaCl then evidence of changes to compactness and oligomeric state (dimer and possibly tetramer) are seen using AUC, but only a single band is apparent on native gels (in contrast to the two bands observed in (12), data not shown). The most extended conformation of cTir-WT was observed at approximately physiological conditions (pH 7.5, 150mM NaCl), while in low salt concentrations (50 mM NaCl) the protein was significantly more compact giving a friction coefficient of 1.21 (averaged value for all species present in solution), indicative of a more globular state. These differences in the compactness of cTir and its oligomerisation state in response to NaCl concentration are not distinguishable by AUC in the context of the full length protein in solution as the distribution of FL-Tir purified in 50mM NaCl is virtually identical to that of protein prepared in 150mM NaCl (data not shown).

Considering the two studies together it would appear that isolated cTir is able to oligomerise, and the oligomerisation state of the protein can be perturbed on phosphorylation but this is dependent on salt concentration. It maybe that preparation at higher salt concentrations (as predominant in this study) is important for ensuring/retaining a monomer conformation as addition of NaCl to 150 mM from samples initially prepared in 50 mM, prior to running native gels, maintains the monomer:dimer equilibrium of cTir (12). However, in 150 mM NaCl buffer a monomer conformation was more readily observed following incubation with PKA (12). These effects suggest that subtle changes in the composition of the cell medium may affect the structural state of Tir and this may have implications for the mechanism of host cell membrane insertion, or downstream signalling.

How does phosphorylation or phosphorylation-mimicking mutations affect the natively unfolded state of cTir/FL-Tir?

All of the 8 cTir variants produced as part of this study and both the native and phosphorylated protein appear to adopt a largely unfolded or loosely packed domain structure in solution. Deconvolution of the CD spectra for the proteins shows a range of 66.2 – 74% ‘unordered’ structure and modelling of the AUC data reveals a frictional coefficient that, when considering the molecular weight of these proteins, translates to a very elongated state that cannot be correlated with a folded domain structure. Also, the proteins all display similar conformational

stability (as assayed by tryptic digest (1ng/µl trypsin) followed SDS-PAGE analysis, data not shown) with a single major breakdown product stable for approximately 15 mins but degraded after 60 mins. The extent of digestion is essentially the same at each time point for all constructs. Despite their unfolded state, the proteins appear stable in solution to high concentrations and show no sign of aggregation up to at least 10mg/ml (monodisperse as observed by dynamic light scattering, single peak on a gel filtration column (well after the void volume), single band on native-PAGE gels (not shown)), the proteins also retain the ability to be phosphorylated by PKA and display changes in apparent molecular mass on SDS-PAGE gels, similar to the full length protein.

Bioinformatic analysis suggests that the phosphorylation-mimicking mutations are on average slightly order promoting (Fig. 5B). This agrees with the experimental data (for instance, the value of the sedimentation coefficient and deconvolution of the CD spectra for the Ser434Asp mutant suggests a more folded and compact structure). Interestingly, the first site (Ser434) for PKA phosphorylation spanning residues Ala424-Ser440 is situated in a region that has MoRF-like properties, as discussed above, while the second site, Ser463, is situated in a disordered region (Thr441-Asp475 (Fig. 5B)). However, it is apparent from the computational and experimental analysis that neither phosphorylation nor the phosphorylation mimicking mutations dramatically affect the structure of the cTir domain in solution. It maybe that cTir requires either the remaining domains of the protein, or a combination of the rest of the protein with the host cell membrane or other factors to refold to a compact state, if indeed it does fold in the context of the intact protein. While cTir itself has some affinity for membranes *in vitro* (7) it is not known whether this forms part of the insertion mechanism; there is no evidence to suggest that cTir can refold on a membrane alone (there is no change in the CD spectra of cTir on incubation with small unilamellar vesicles mimicking the lipid composition of the host-cell membrane (data not shown)).

As for the cTir domain, AUC reveals FL-Tir does not undergo any major structural rearrangements following modification of Ser434/Ser463 by phosphorylation or mutagenesis. This shows that the subtle changes observed by CD are not linked to large scale changes in tertiary structure. Phosphorylation does appear to stabilise a higher molecular weight component of FL-Tir in solution (peak at ~4 S, 10 % rather than 3% in the native protein, Fig. 3C), but it is not known at present whether this is an oligomeric state of the protein or non-specific aggregation. In either case this component is a minor species in solution. The conformational stability of FL-Tir does not appear to be significantly affected by modification at residues 434/463, as determined by tryptic digest (1ng/µl trypsin) data not shown).

In summary, this study aimed to determine the effects of site directed mutagenesis at previously identified serine phosphorylation sites on the structure of the EPEC virulence protein Tir. It has been shown that both the isolated cTir domain and the FL-Tir protein appear to be natively unfolded in solution, and modification of the targeted residues has little effect on the structures (be it enzymatic phosphorylation or mutagenesis) at physiological NaCl concentrations. It still remains plausible that phosphorylation of these residues has a role in the mechanism of membrane insertion or promoting structural rearrangements post-insertion through either charge effects, recognition of accessory factors (or both) or other, as yet unidentified downstream signalling activities. The recognition of Tir adopting a natively unfolded state in solution has importance for directing further structural studies (for instance, the fact it is not suitable for X-ray crystallographic study). At present low-resolution, solution-based approaches appear to be the most appropriate way to investigate the structure of Tir, both in the aqueous phase and inserted into the membrane.

Acknowledgements

This work was funded by the Royal Society (UK) through the award of a University Research Fellowship to MJB. MJB and ASS also thank the University of Newcastle for financial support, Brendan Kenny for discussion, Dave Scott (University of Nottingham, UK) for initial AUC data and Duncan McNulty for technical help.

Abbreviations

Tir, translocated intimin receptor; FL-Tir, full length-Tir; cTir, C-terminal domain of Tir; CD, circular dichroism; AUC, analytical ultracentrifugation; SV, sedimentation velocity; EPEC, enteropathogenic *E. coli*; TTSS, type three secretion system; ATP adenosine tri-phosphate; PKA, protein kinase A (cAMP-dependent protein kinase).

References

1. Nataro, J. P., and J. B. Kaper. 1998. Diarrheagenic Escherichia coli. Clin Microbiol Rev 11:142-201.
2. Kenny, B. 2002. Enteropathogenic Escherichia coli (EPEC)-- a crafty subversive little bug. Microbiology 148:1967-1978.
3. Vallance, B. A., and B. B. Finlay. 2000. Exploitation of host cells by enteropathogenic Escherichia coli. Proc Natl Acad Sci U S A 97:8799-8806.
4. Kenny, B., R. DeVinney, M. Stein, D. J. Reinscheid, E. A. Frey, and B. B. Finlay. 1997. Enteropathogenic E. coli (EPEC) transfers its receptor for intimate adherence into mammalian cells. Cell 91:511-520.
5. Kenny, B. 1999. Phosphorylation of tyrosine 474 of the enteropathogenic Escherichia coli (EPEC) Tir receptor molecule is essential for actin nucleating activity and is preceded by additional host modifications. Mol Microbiol 31:1229-1241.
6. de Grado, M., A. Abe, A. Gauthier, O. Steele-Mortimer, R. DeVinney, and B. B. Finlay. 1999. Identification of the intimin-binding domain of Tir of enteropathogenic Escherichia coli. Cell Microbiol 1:7-17.
7. Race, P. R., J. H. Lakey, and M. J. Banfield. 2006. Insertion of the enteropathogenic Escherichia coli Tir virulence protein into membranes in vitro. J Biol Chem 281:7842-7849.
8. Campellone, K. G., A. Giese, D. J. Tipper, and J. M. Leong. 2002. A tyrosine-phosphorylated 12-amino-acid sequence of enteropathogenic Escherichia coli Tir binds the host adaptor protein Nck and is required for Nck localization to actin pedestals. Mol Microbiol 43:1227-1241.
9. Gruenheid, S., R. DeVinney, F. Bladt, D. Goosney, S. Gelkop, G. D. Gish, T. Pawson, and B. B. Finlay. 2001. Enteropathogenic E. coli Tir binds Nck to initiate actin pedestal formation in host cells. Nat Cell Biol 3:856-859.
10. Campellone, K. G., and J. M. Leong. 2005. Nck-independent actin assembly is mediated by two phosphorylated tyrosines within enteropathogenic Escherichia coli Tir. Mol Microbiol 56:416-432.
11. Warawa, J., and B. Kenny. 2001. Phosphoserine modification of the enteropathogenic Escherichia coli Tir molecule is required to trigger conformational changes in Tir and efficient pedestal elongation. Mol Microbiol 42:1269-1280.
12. Hawrani, A., C. E. Dempsey, M. J. Banfield, D. J. Scott, A. R. Clarke, and B. Kenny. 2003. Effect of protein kinase A-mediated phosphorylation on the structure and association properties of the enteropathogenic Escherichia coli Tir virulence protein. J Biol Chem 278:25839-25846.
13. Huffine, M. E., and J. M. Scholtz. 1996. Energetic implications for protein phosphorylation. Conformational stability of HPr variants that mimic phosphorylated forms. J Biol Chem 271:28898-28902.
14. Jang, Y. J., S. Ma, Y. Terada, and R. L. Erikson. 2002. Phosphorylation of threonine 210 and the role of serine 137 in the regulation of mammalian polo-like kinase. J Biol Chem 277:44115-44120.
15. Leger, J., M. Kempf, G. Lee, and R. Brandt. 1997. Conversion of serine to aspartate imitates phosphorylation-induced changes in the structure and function of microtubule-associated protein tau. J Biol Chem 272:8441-8446.

16. Receveur-Brechot, V., J. M. Bourhis, V. N. Uversky, B. Canard, and S. Longhi. 2006. Assessing protein disorder and induced folding. Proteins 62:24-45.
17. Uversky, V. N. 2002. What does it mean to be natively unfolded? Eur J Biochem 269:2-12.
18. Uversky, V. N., J. R. Gillespie, I. S. Millett, A. V. Khodyakova, R. N. Vasilenko, A. M. Vasiliev, I. L. Rodionov, G. D. Kozlovskaya, D. A. Dolgikh, A. L. Fink, S. Doniach, E. A. Permyakov, and V. M. Abramov. 2000. Zn(2+)-mediated structure formation and compaction of the "natively unfolded" human prothymosin alpha. Biochem Biophys Res Commun 267:663-668.
19. Li, J., V. N. Uversky, and A. L. Fink. 2002. Conformational behavior of human alpha-synuclein is modulated by familial Parkinson's disease point mutations A30P and A53T. Neurotoxicology 23:553-567.
20. Uversky, V. N. 2002. Natively unfolded proteins: a point where biology waits for physics. Protein Sci 11:739-756.
21. Sanchez-Puig, N., D. B. Veprintsev, and A. R. Fersht. 2005. Human full-length Securin is a natively unfolded protein. Protein Sci 14:1410-1418.
22. Batra-Safferling, R., K. Abarca-Heidemann, H. G. Korschen, C. Tziatzios, M. Stoldt, I. Budyak, D. Willbold, H. Schwalbe, J. Klein-Seetharaman, and U. B. Kaupp. 2006. Glutamic acid-rich proteins of rod photoreceptors are natively unfolded. J Biol Chem 281:1449-1460.
23. Brown, P. H., and P. Schuck. 2006. Macromolecular size-and-shape distributions by sedimentation velocity analytical ultracentrifugation. Biophys J 90:4651-4661.
24. Sambrook, J., and D. W. Russell. 2001. Molecular Cloning. A manual, 3rd Edition.
25. Whitmore, L., and B. A. Wallace. 2004. DICHROWEB, an online server for protein secondary structure analyses from circular dichroism spectroscopic data. Nucleic Acids Res 32:W668-673.
26. Provencher, S. W., and J. Glockner. 1981. Estimation of globular protein secondary structure from circular dichroism. Biochemistry 20:33-37.
27. Laue, T. M., B. D. Shah, T. M. Ridgeway, and S. Pelletier. 1992. Analytical ultracentrifugation in Biochemistry and polymer science. Redwood Press Ltd., Melksham.
28. Durchschlag, H. 1986. Specific volumes of macromolecules and some other molecules of biological interest. In Thermodynamic data for Biochemistry and Biotechnology. H.-J. Hinz, editor. Springer-Verlag, Berlin-Heidelberg-New York-Tokyo. 45-128.
29. Schuck, P. 2000. Size-distribution analysis of macromolecules by sedimentation velocity ultracentrifugation and lamm equation modeling. Biophys J 78:1606-1619.
30. Lamm, O. 1929. Die Differentialgleichung der Ultrazentrifugierung. Ark. Mat. Astr. Fys. 21B:1-4.
31. Schuck, P. 1998. Sedimentation analysis of noninteracting and self-associating solutes using numerical solutions to the Lamm equation. Biophys J 75:1503-1512.
32. Schuck, P. 2003. On the analysis of protein self-association by sedimentation velocity analytical ultracentrifugation. Anal Biochem 320:104-124.

33. Dam, J., and P. Schuck. 2004. Calculating sedimentation coefficient distributions by direct modeling of sedimentation velocity concentration profiles. Methods Enzymol 384:185-212.
34. Romero, P., Z. Obradovic, X. Li, E. C. Garner, C. J. Brown, and A. K. Dunker. 2001. Sequence complexity of disordered protein. Proteins 42:38-48.
35. Lebowitz, J., M. S. Lewis, and P. Schuck. 2002. Modern analytical ultracentrifugation in protein science: a tutorial review. Protein Sci 11:2067-2079.
36. Tompa, P. 2002. Intrinsically unstructured proteins. Trends Biochem Sci 27:527-533.
37. Stapley, B. J., and T. P. Creamer. 1999. A survey of left-handed polyproline II helices. Protein Sci 8:587-595.
38. Fink, A. L. 2005. Natively unfolded proteins. Curr Opin Struct Biol 15:35-41.
39. Uversky, V. N., C. J. Oldfield, and A. K. Dunker. 2005. Showing your ID: intrinsic disorder as an ID for recognition, regulation and cell signaling. J Mol Recognit 18:343-384.
40. Oldfield, C. J., Y. Cheng, M. S. Cortese, P. Romero, V. N. Uversky, and A. K. Dunker. 2005. Coupled folding and binding with alpha-helix-forming molecular recognition elements. Biochemistry 44:12454-12470.
41. Mohan, A., C. J. Oldfield, P. Radivojac, V. Vacic, M. S. Cortese, A. K. Dunker, and V. N. Uversky. 2006. Analysis of molecular recognition features (MoRFs). J Mol Biol 362:1043-1059.
42. Belmont, L., T. Mitchison, and H. W. Deacon. 1996. Catastrophic revelations about Op18/stathmin. Trends Biochem Sci 21:197-198.
43. Campbell, K. M., A. R. Terrell, P. J. Laybourn, and K. J. Lumb. 2000. Intrinsic structural disorder of the C-terminal activation domain from the bZIP transcription factor Fos. Biochemistry 39:2708-2713.
44. Ptitsyn, O. 1995. Molten globule and protein folding. Advances in Protein Chemistry 47:83-229.
45. Nimmo, G. A., and P. Cohen. 1978. The regulation of glycogen metabolism. Purification and characterisation of protein phosphatase inhibitor-1 from rabbit skeletal muscle. Eur J Biochem 87:341-351.
46. Hemmings, H. C., Jr., A. C. Nairn, D. W. Aswad, and P. Greengard. 1984. DARPP-32, a dopamine- and adenosine 3':5'-monophosphate-regulated phosphoprotein enriched in dopamine-innervated brain regions. II. Purification and characterization of the phosphoprotein from bovine caudate nucleus. J Neurosci 4:99-110.
47. Uversky, V. N. 1993. Use of fast protein size-exclusion liquid chromatography to study the unfolding of proteins which denature through the molten globule. Biochemistry 32:13288-13298.
48. Wiesner, B., J. Weiner, R. Middendorff, V. Hagen, U. B. Kaupp, and I. Weyand. 1998. Cyclic nucleotide-gated channels on the flagellum control Ca2+ entry into sperm. J Cell Biol 142:473-484.
49. Josefsson, E., D. O'Connell, T. J. Foster, I. Durussel, and J. A. Cox. 1998. The binding of calcium to the B-repeat segment of SdrD, a cell surface protein of Staphylococcus aureus. J Biol Chem 273:31145-31152.

Table 1. Secondary structure components of cTir and FL-Tir as determined by deconvolution of CD spectra (average of separate calculations using CONTIN, CDSSTR and SELCON3). [a]number of residues adopting this secondary structure in the protein (based on a total of 165 residues in cTir and 550 residues in FL-Tir). [#] ref. 12.

	α-Helix		β-Strand		Turn		Unordered	
	%	n^a	%	n^a	%	n^a	%	n^a
cTir WT (150 mM NaCl)	9.9	16	8.2	14	10.3	17	71.8	118
cTir WT (50 mM NaCl)	10.4	17	7.1	12	9.5	16	73.0	120
cTir WT-P	13.4	22	9.4	16	9.2	15	68.0	112
cTir 434A	7.2	12	8.1	14	14.2	23	70.5	116
cTir 434D	10.1	17	7.9	13	12.6	21	69.4	114
cTir 463A	8.7	14	7.2	12	10.6	17	73.5	122
cTir 463D	13.3	22	9.7	16	10.8	18	66.2	109
cTir 434A/463D	14.4	24	8.3	14	10.5	17	66.8	110
cTir 434D/434A	9.8	16	8.7	14	11.2	18	70.3	117
cTir 434A/463A	8.8	15	7.4	12	10.2	17	74.0	121
cTir 434D/463D	13.6	22	8.9	15	9.6	16	67.9	112
FL-Tir WT	20.9	115	24.3	134	22.0	121	32.2	188
FL-Tir WT (50 mM NaCl)[#]	25.8	142	23.3	117	21.5	107	29.0	159
FL-Tir WT-P	24.4	134	24.8	136	23.1	127	27.7	153
FL-Tir 434D/463D	25.1	138	23.9	131	22.5	124	28.5	154

Table 2. Hydrodynamic parameters for cTir/FL-Tir derived from AUC experiments (interference data)

	Sedimentation coefficient (S)			Mass (kDa)			Hydrodynamic radius (Å)
	s1	s2	s3	M1	M2	M3	Rs
cTir WT (150 mM NaCl)	1.20±0.01	—	—	19.6±0.4	—	—	38.8±0.2
cTir WT (50 mM NaCl)	1.78±0.10	2.61±0.14	4.22±0.1	18.5±0.5	39.7±2.1	68.2±2.2	—
cTir WT-P	1.47±0.01	—	—	19.3±0.4	—	—	35.4±0.5
cTir 434A	1.48±0.08	—	—	20.3±0.4	—	—	37.4±0.3
cTir 434D	1.52±0.03	—	—	19.5±0.4	—	—	35.0±0.9
cTir 463A	1.48±0.02	—	—	20.5±0.5	—	—	37.0±0.7
cTir 463D	1.49±0.04	—	—	18.1±0.4	—	—	33.8±0.4
cTir 434A/463D	1.48±0.01	—	—	20.5±0.2	—	—	37.3±0.4
cTir 434D/463A	1.50±0.01	—	—	19.9±0.2	—	—	36.2±0.3
cTir 434A/463A	1.46±0.02	—	—	17.7±0.7	—	—	33.8±0.8
cTir 434D/463D	1.47±0.02	—	—	19.5±0.5	—	—	34.7±1.2
FL-Tir WT (150 mM NaCl)	2.65±0.01	—	—	60.5±2.1	—	—	57.0±0.6
FL-Tir WT (50 mM NaCl)	2.67±0.02			58.4±2.6			54.32±2.9
FL-Tir WT-P	2.68±0.03	—	—	58.5±2.5	—	—	56.2±2.4
FL-Tir 434D/463D	2.65±0.03	—	—	61.9±1.4	—	—	62.7±0.7

Table 3. Hydrodynamic characteristics of cTir/FL-Tir compared to other natively/urea-unfolded proteins.

		Mass, (kDa)	Hydrodynamic radius (Å)	Ref.
cTir WT (150 mM NaCl)		19.8	38.8±0.2	
Natively unfolded proteins	Stathmin	17	33	(42)
	CFos-AD domain, 216-380 fragment	17.3	35	(43)
	Calf thymus histone	19.8	36.7	(44)
	PPI-1	20.8	32.3	(45)
	Securin	22.2	39.7	(21)
	DARPP-32	23.1	34	(46)
	β-Casein	24	41.7	(44)
8M urea unfolded proteins without crosslinks	Myoglobin	16.9	35.1	(47)
	β-Lactoglobulin	18.5	37.8	(47)
	Chymotrypsinogen	25.7	45	(47)
FL-Tir WT		59.2	57.0±0.6	
Natively unfolded proteins	Taka-amylase A, reduced	52.5	43.1	(44)
	GARP1	64.5	65	(48)
	SdrD protein B1-B5 fragment	64.8	54.7	(49)
8M urea unfolded proteins without crosslinks	Serum albumin	66.3	74	(47)

Figure Legends.

Fig. 1. 12% SDS-PAGE gel of cTir WT and Ala/Asp mutant proteins. WT refers to the wild type protein. Ala and Asp residues are referred to by their residue number and single letter code. 8 ng of protein was loaded in each lane and samples were visualised by Coomassie Blue staining.

Fig 2. SDS-PAGE gels showing the effects of phosphorylation on (A) the Ala mutants, (B) the Asp mutants and (C) the Ala/Asp combinations in cTir and (D) FL-Tir. cTir samples were run on 12% gels, FL-Tir samples on 8% gels. WT refers to the wild type protein. Ala and Asp residues are referred to by their single letter code. Phosphorylation assays were performed as described in materials and methods. 8 ng of cTir and 10ng of FL-Tir were loaded in each lane as appropriate and samples were visualised by Coomassie Blue staining.

Fig. 3. General size distribution (c(s)) analysis of the SV data converted to standard conditions for (A) cTir WT in 150 mM NaCl, c = 0.92 mg/ml (solid line), Ser434Asp/Ser463Asp mutant, c= 1 mg/ml (dashed line) and phosphorylated sample, c= 0.92 mg/ml (dotted line); (B) cTir in 50mM NaCl, the sample concentrations were ranged from 0.3 mg/ml to 1.4 mg/ml; in the insert: linear extrapolation to zero concentrations s_w for each detected species (monomer (□), dimer (○), tetramer (Δ), dashed lines) and weight-average s for all three species together (*, solid line); (C) FL-Tir, the samples and symbols as in (A). The concentrations were WT – 1.2 mg/ml; Ser434Asp/Ser463Asp mutant - 0.87 mg/ml, phosphorylated protein - 0.85 mg/ml.

Fig. 4. Far-UV Circular Dichroism. (A) Wavelength scans of cTir WT and mutants. The data displays two overall patterns, as discussed in the text. In black are traces for WT, Ser434Asp, Ser463Ala, Ser463Asp, Ser434Ala/Ser463Ala and Ser434Ala/Ser463Asp; in gray: Ser434Ala, Ser434Asp/S463Ala and Ser434Asp/Ser463Asp. (B) Wavelength scans for full length protein (solid line = WT, dashed line = Ser434Asp/Ser463Asp).

Figure 5. PONDR prediction for intrinsic disorder from amino acid sequences (A) FL-Tir, (B) cTir WT (solid line), Ser434Asp/Ser463Asp (dashed line), Ser434Ala/Ser463Ala (dotted line). The predicted MoRF sequence, as discussed in the text, is shown as a hashed box.

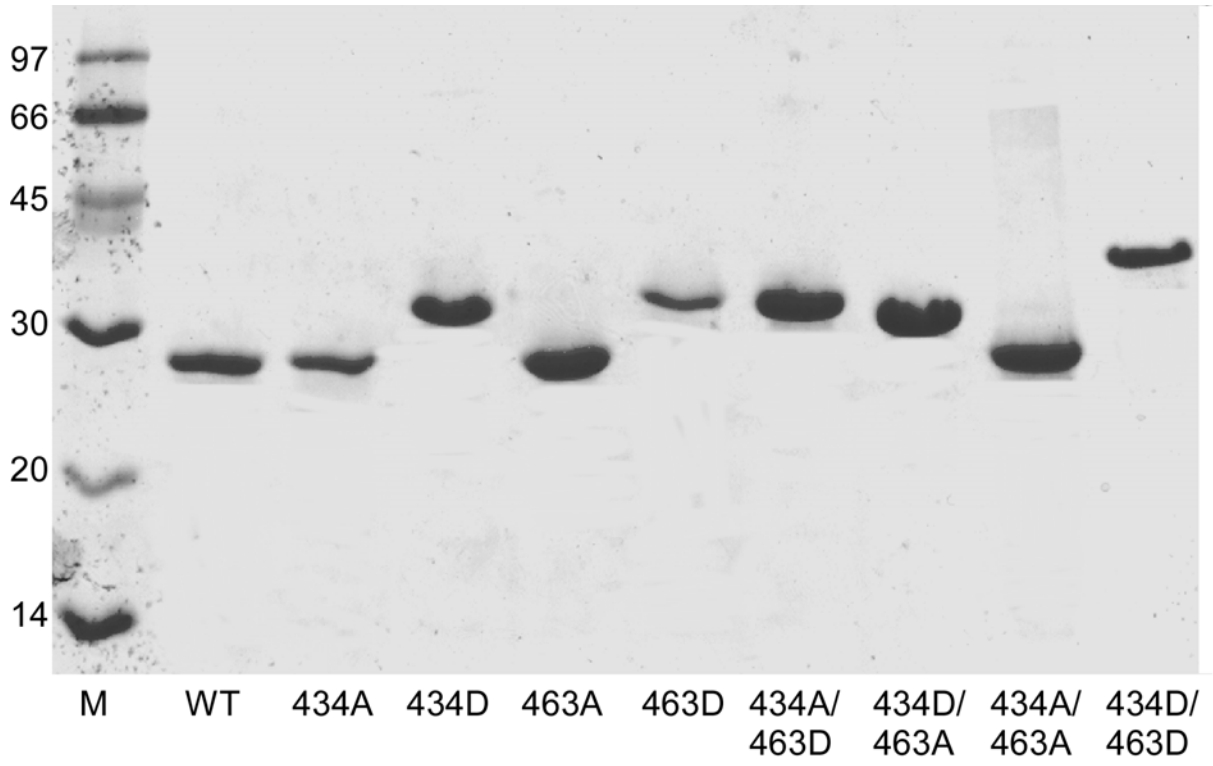
97
66
45
30
20
14
M
WT
434A
434D
463A
463D
434A/
463D
434D/
463A
434A/
463A
434D/
463D

Figure 1

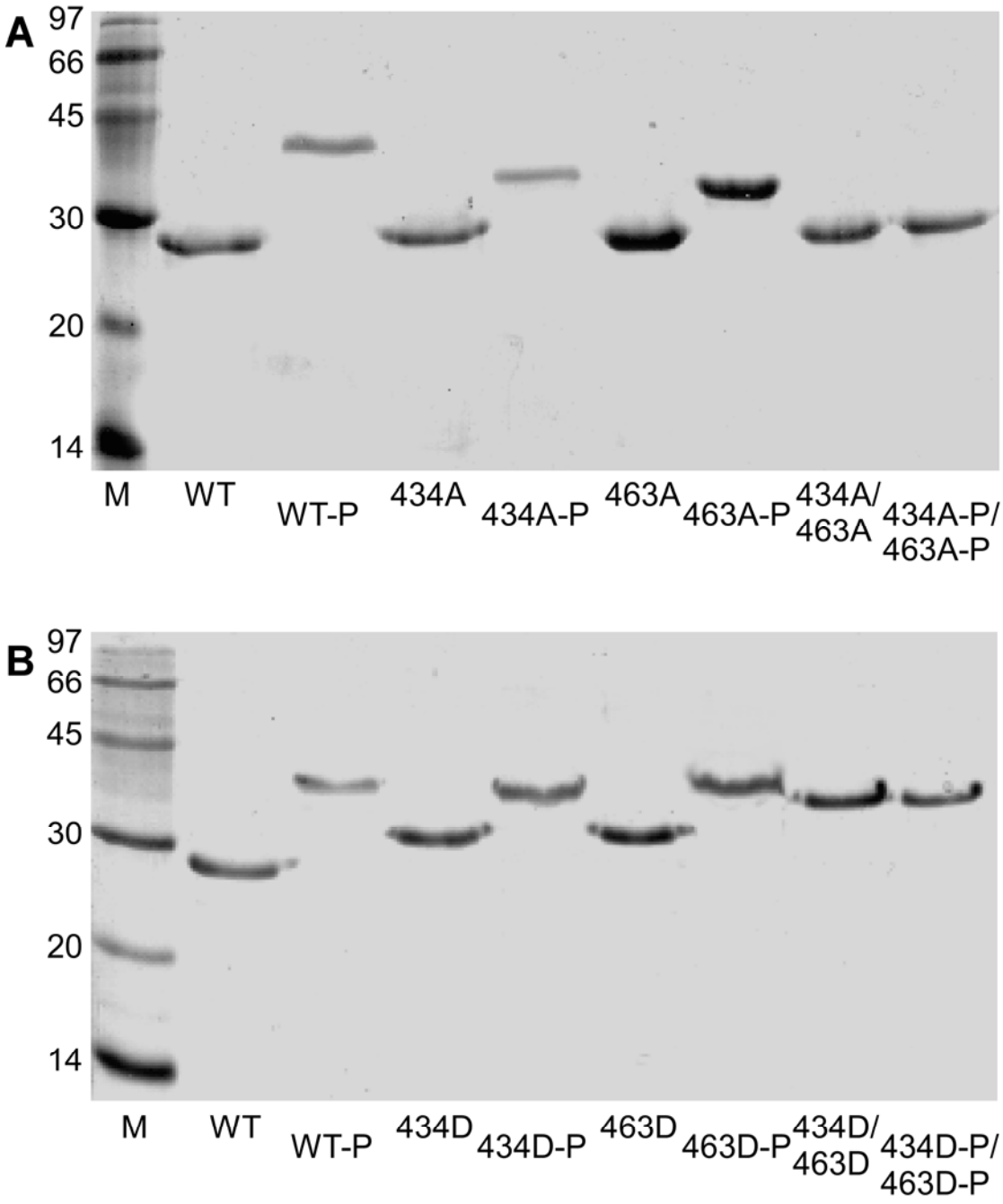
A
97
66
45
30
20
14
M
WT
WT-P
434A
434A-P
463A
463A-P
434A/
463A
434A-P/
463A-P
B
97
66
45
30
20
14
M
WT
WT-P
434D
434D-P
463D
463D-P
434D/
463D
434D-P/
463D-P

Figure 2

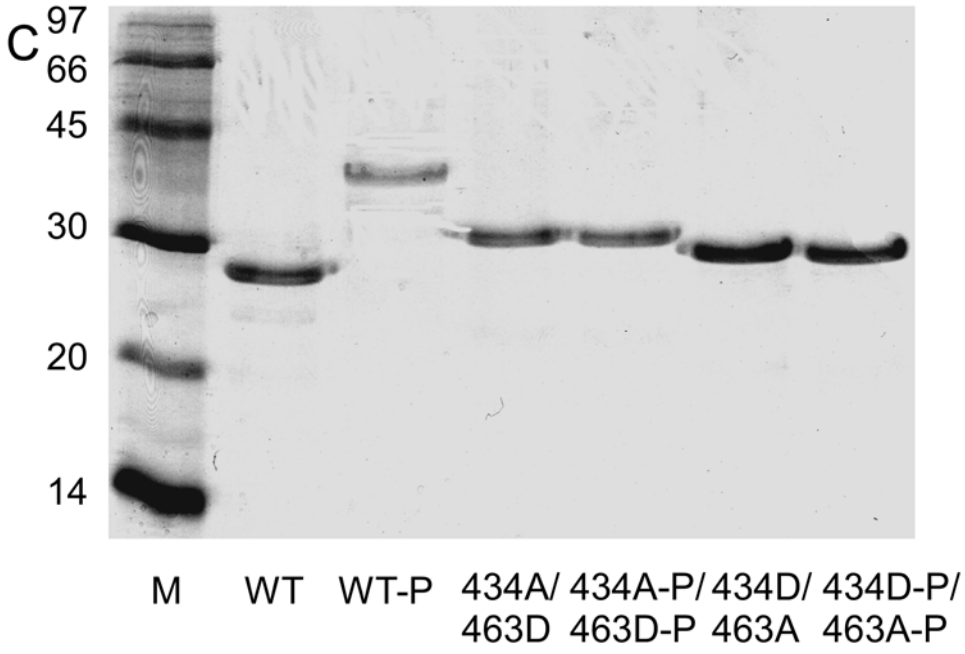
C
97
66
45
30
20
14
M
WT
WT-P
434A/ 463D
434A-P/ 463D-P
434D/ 463A
434D-P/ 463A-P

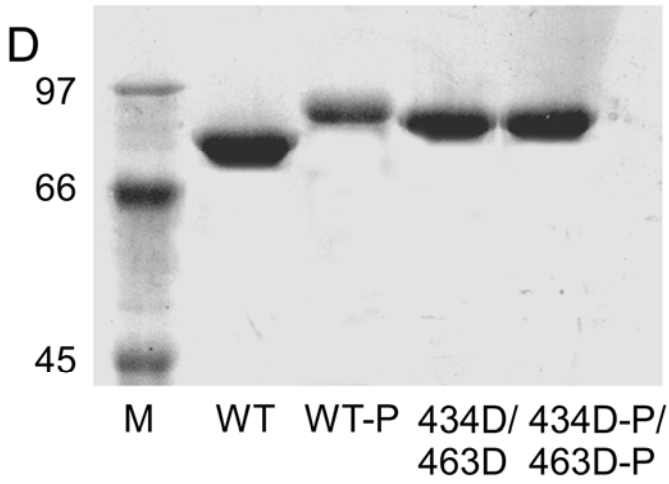
D
97
66
45
M
WT
WT-P
434D/ 463D
434D-P/ 463D-P

Figure 2

A

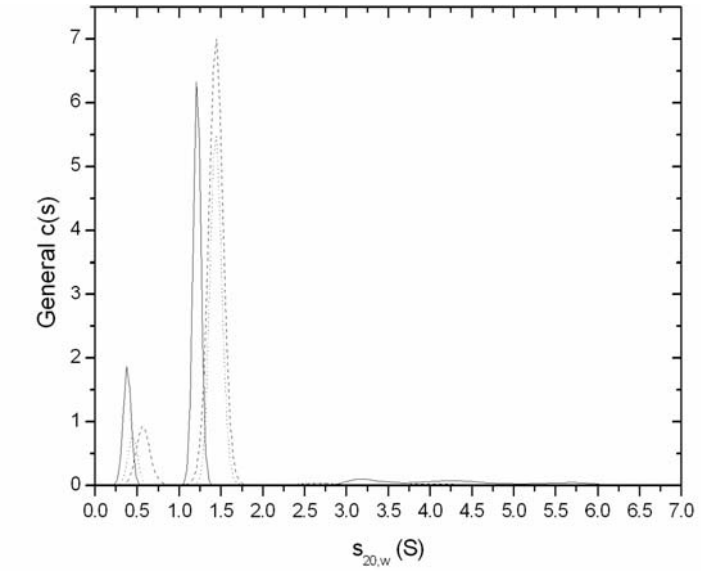
General c(s)
$s_{20,w}$ (S)

B

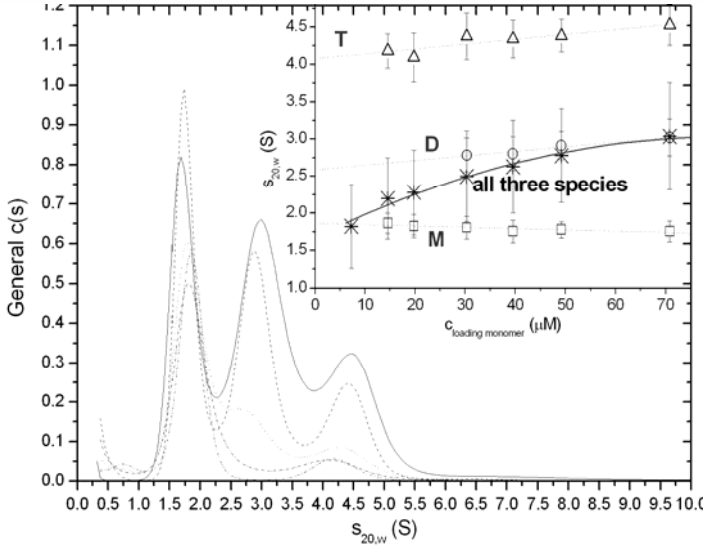
General c(s)
$s_{20,w}$ (S)
T
D
M
all three species
$s_{20,w}$ (S)
$c_{loading\ monomer}$ (μM)

C

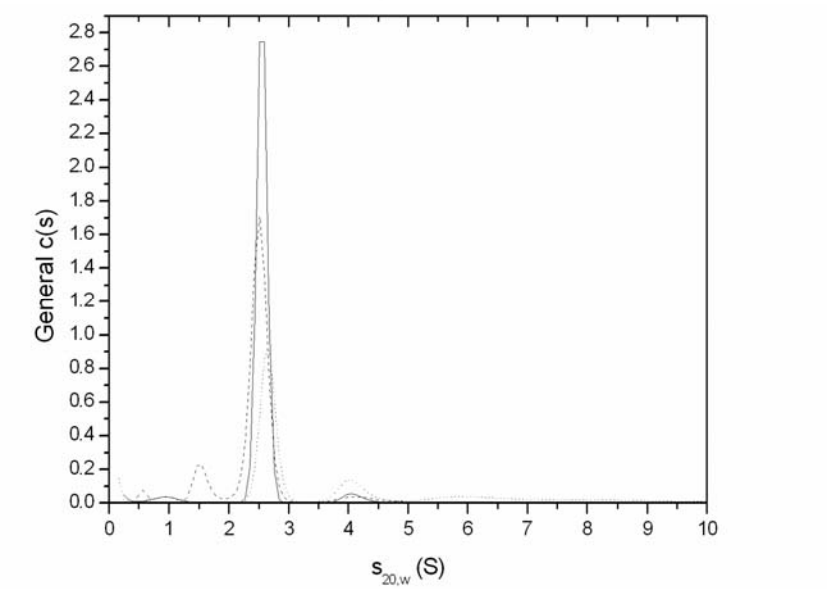
General c(s)
$s_{20,w}$ (S)

Figure 3

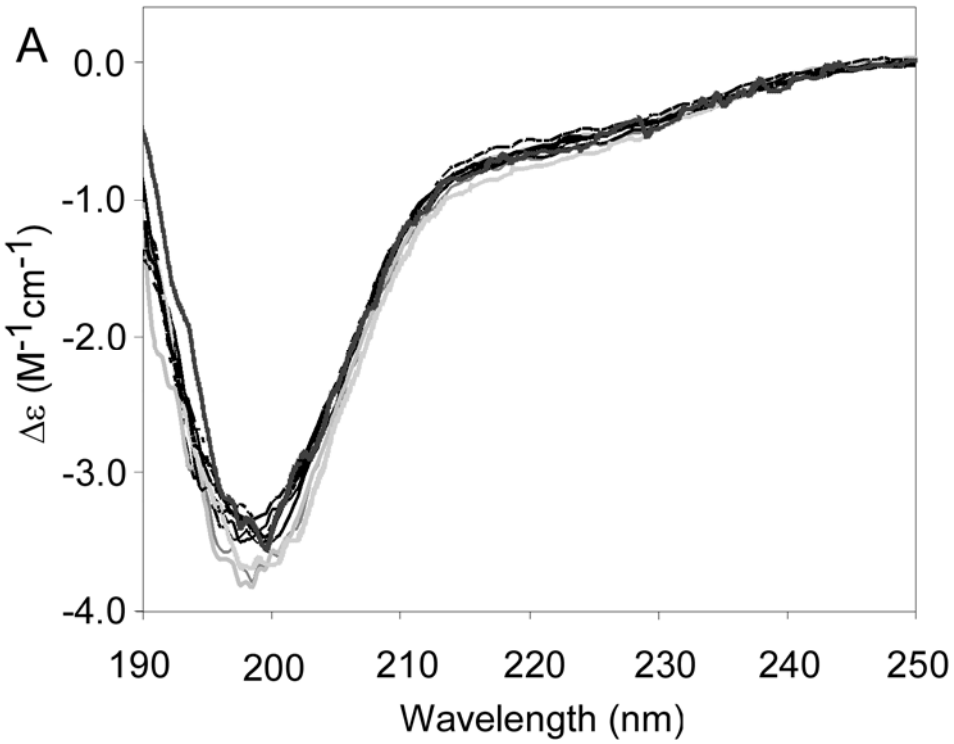
A
0.0
-1.0
-2.0
-3.0
-4.0
Δε (M-1cm-1)
190
200
210
220
230
240
250
Wavelength (nm)

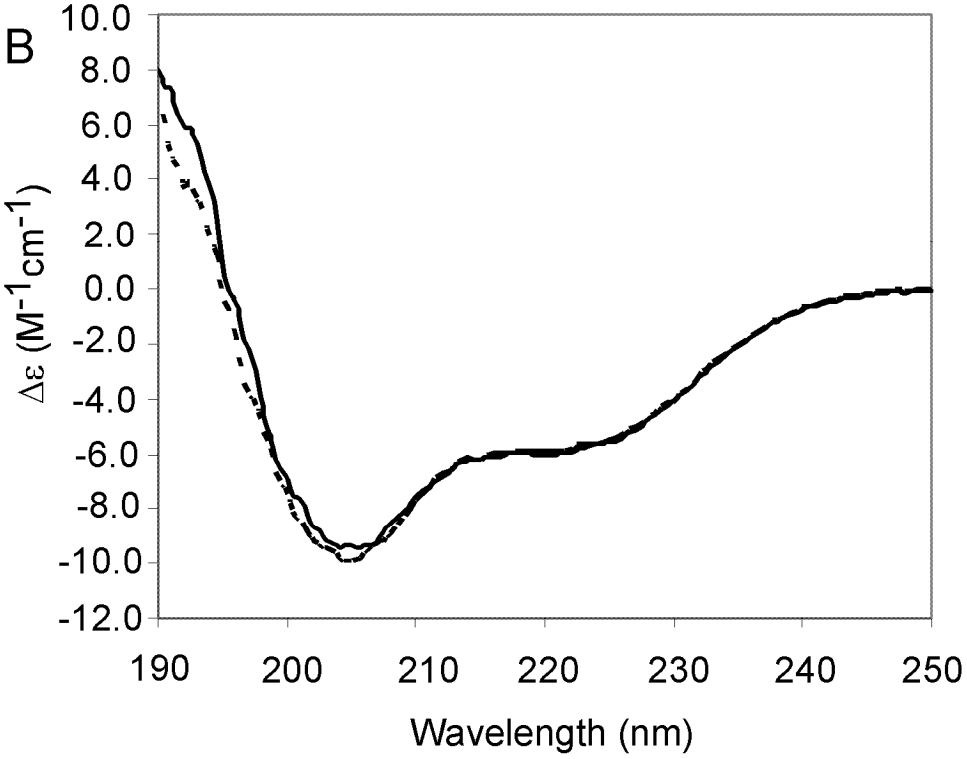
B
10.0
8.0
6.0
4.0
2.0
0.0
-2.0
-4.0
-6.0
-8.0
-10.0
-12.0
Δε (M-1cm-1)
190
200
210
220
230
240
250
Wavelength (nm)

Figure 4

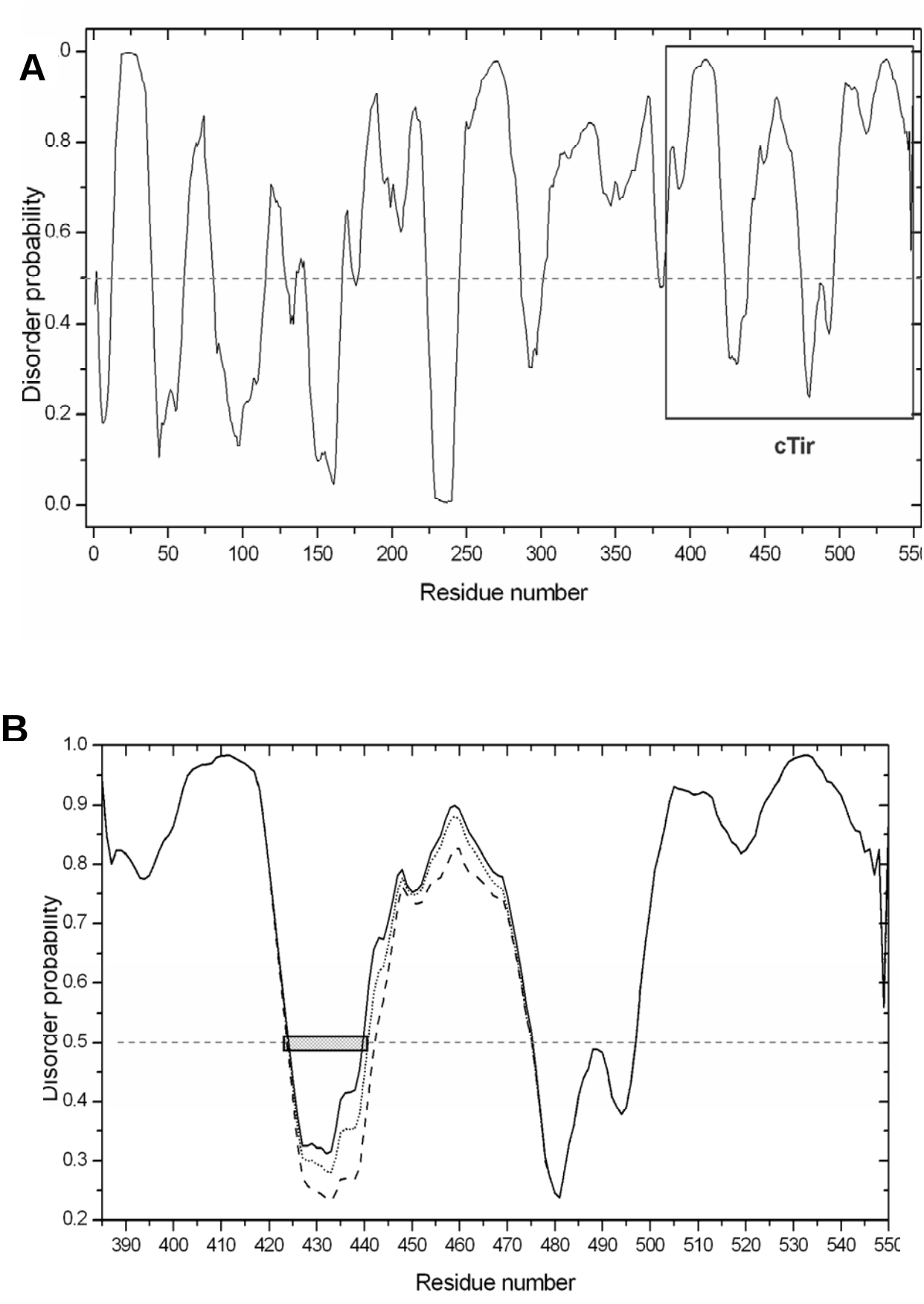
A
Disorder probability
0.0
0.2
0.4
0.6
0.8
0
50
100
150
200
250
300
350
400
450
500
Residue number
cTir
B
Disorder probability
0.2
0.3
0.4
0.5
0.6
0.7
0.8
0.9
1.0
390
400
410
420
430
440
450
460
470
480
490
500
510
520
530
540
Residue number

Figure 5